



Paclitaxel-clusters coated with hyaluronan as selective tumor-targeted nanovectors

Ilia Rivkin^{a,1}, Keren Cohen^{b,c}, Jacob Koffler^{a,2}, Dina Melikhov^a, Dan Peer^{b,c,1,3,*}, Rimona Margalit^{a,c,**}

^aDepartment of Biochemistry and Molecular Biology, George S. Wise Faculty of Life Sciences, Israel

^bLaboratory of Nanomedicine, Department of Cell Research and Immunology, George S. Wise Faculty of Life Sciences, Israel

^cCenter for Nanoscience and Nanotechnology, Tel Aviv University, Tel Aviv 69978, Israel

ARTICLE INFO

Article history:

Received 30 April 2010

Accepted 25 May 2010

Available online 17 June 2010

Keywords:

Paclitaxel

Drug delivery

Tumor targeting

Hyaluronan

Abraxane

ABSTRACT

Paclitaxel (PTX) is a widely used anti-tumor agent in the treatment of solid tumors. Lack of selective strategies to target PTX into tumor cells together with poor solubility necessitating detergent, are severe clinical limitations. To address these hurdles, we devised a strategy that utilized PTX insolubility, mixing it with lipids that self-assemble into nanoparticle-like clusters. These clusters were then coated with hyaluronan, a glycosaminoglycan (GAG), and termed PTX-GAGs. These particles, delivered PTX selectively into tumor cells in a CD44-dependent manner. Injected systemically to mice bearing solid tumors, the PTX-GAGs showed high safety profile and tumor accumulation. Tumor progression was exponential upon treatment with free PTX or PTX in albumin nanoparticles (the FDA-approved Taxol® and Abraxane®, respectively). Under the same conditions, PTX-GAGs induced tumor arrest and were as potent as a 4-fold higher Taxol® dose. Our findings suggest GAGs merit further investigation as vehicles for taxanes, and may be applicable as carriers in other therapeutic settings.

© 2010 Elsevier Ltd. All rights reserved.

1. Introduction

Paclitaxel (PTX), a microtubules stabilizer that causes mitotic arrest, has shown broad-spectrum activity in many solid tumors including ovarian, breast, AIDS-related Kaposi's sarcoma, lung, head and neck and bladder [1,2]. The FDA-approved formulation of PTX-Cre (Taxol®), requires dissolving the paclitaxel in Cremophor® EL (polyoxyethylated castor oil) and ethanol (CrEL) [3]. However, the use of Taxol® requires premedication with corticosteroids and antihistamines to reduce risks of hypersensitivity reaction [4–7]. It can also cause neutropenia [8], and prolonged, peripheral neuropathy, which may be associated with axonal degradation [6,7]. In addition to serious toxicities, CrEL may negatively impact efficacy by limiting tumor penetration through the formation of

large polar micelles, which can lead to nonlinear pharmacokinetics and decreased unbound drug fraction [6,8].

Among carriers for paclitaxel made from biological materials, liposomes have been well-studied as carriers for PTX, although drug loading into liposomes is relatively low ($\leq 10\%$ (w/w)) [9–14]. Recently, a new formulation was approved by the FDA, albumin-bound PTX (nab™-PTX; Abraxane®) forming nanoparticles (~ 135 nm in diameter). This formulation, consisting of unmodified PTX and human albumin, is CrEL-free. By eliminating CrEL from its formulation, nab-PTX reduces risks of hypersensitivity reactions, does not require premedication, and can be given over a shorter period without special intravenous tubing [15]. However, it is reported to have low PTX loading yield, similar to liposomes and minimal improvement in efficacy [16]. Both liposomes and nab™-PTX are non-targeted drug carriers that utilize the enhanced permeability and retention effect (EPR) [17,18] to accumulate at close proximity to the tumors.

The frequent overexpression of the hyaluronan (HA) receptors CD44 and CD168 (RHAMM) on many types of tumors opens new avenues for targeting by the naturally-occurring high-molecular weight HA [19–22]. HA, a naturally-occurring glycosaminoglycan, is one of the major components of the extracellular matrix (ECM). It is found in many tissues such as skin, joint tissue (in synovial fluid) and eyes [23,24]. HA is known as a bioadhesive compound capable of binding with high affinity to both cell surface and intracellular

* Corresponding author. Laboratory of Nanomedicine, Department of Cell Research and Immunology, Tel Aviv University, Tel Aviv 69978, Israel. Tel.: +972 3640 7925; fax: +972 3640 5926.

** Corresponding author. Department of Biochemistry and Molecular Biology, Tel Aviv University, Tel Aviv 69978, Israel. Tel.: +972 3 6409822; fax: +972 3 5406834.

E-mail addresses: peer@post.tau.ac.il (D. Peer), rimona@post.tau.ac.il (R. Margalit).

¹ IR and DP contributed equally to this study.

² Present address: Department of Biomedical Engineering, Technion, Israel

³ Former affiliation: Immune Disease Institute, Harvard Medical School, Boston 02115, Massachusetts, USA

receptors, to ECM components and to itself [25,26]. In cancer cells, binding of HA to its receptors is involved in tumor growth and spreading. CD44 regulates cancer cells proliferation and metastatic processes [27,28]. In addition, disruption of HA–CD44 binding was shown to reduce tumor progression [29–31]. Administration of exogenous HA resulted in arrest of tumor spreading [31]. HA is a non-toxic and non-immunogenic compound, already approved for use in eye surgery, joint therapy and wound healing [32]. Coating small unilamellar liposomes with HA stabilizes these particles in a cycle of lyophilization and rehydration [33], provides selective targeting to tumors expressing the HA receptors [19,20,34], and presents a scaffold for conjugation of other ligands to the surface for further improving the selectivity to cell surface receptors [35].

Here, we report on tumor-targeted nanoparticles, constructed of PTX-phosphatidylethanolamine (PE) clusters covalently coated with HA. The terms used for the particles themselves (i.e., drug-free) and when loaded with PTX are GAGs and PTX-GAGs, respectively [36]. In contrast to other phospholipids such as phosphatidylcholine (PC) or phosphatidylserine (PS) that form lipid bilayers closed into circular particle like liposomes, PE by itself does not form a liposome, but other lamellar shapes. The variety of shapes depends on several factors such as the lipid side chains, concentration, temperature, pressure, hydration level, pH, and salt concentration [37–42]. For the present task we selected dilauroyl-PE (DLPE). The saturated chains are more stable than unsaturated chains that tend to oxidize into toxic peroxi-lipids. Being relatively-short, the DL chains impart additional advantages: (i) relatively low gel-liquid crystalline transition temperature ($T_m = 43\text{ }^\circ\text{C}$) [43], indicating homogenous particle suspensions may be achieved without the need for over-heating that may harm incorporated drugs, and (ii) higher affinity, compared to longer chains, to PTX [14,44].

Herein, we report studies at the molecular, cellular and whole animal levels of organization. The molecular studies included preparation, physicochemical, thermal analyses and ultrastructure characterization of the PTX-GAG particles. The *in vitro* studies in cancer cells included GAGs-cell binding and internalization, as well the cytotoxicity of PTX-GAGs. Biological effects of the PTX-GAG particles, studied in BALB/c mice, included evaluations of liver enzyme release and inductions of cytokines and of interferon response. PTX-GAGs retention in circulation, biodistribution, weight changes and efficacy were studied in BALB/c mice bearing a solid s.c. tumor (CT-26). Control systems were usually saline, drug-free GAGs and Taxol, and the addition of Abraxane[®] for the *in vivo* efficacy studies.

2. Materials and methods

2.1. Materials

2.1.1. Cell lines

Cell monolayers (all were purchased from American Type Culture Collection (ATCC)) were grown in 100×20 mm dishes (culture plates and dishes were from Corning, Corning Glass works, Corning, New York, USA). The CT-26 and D122 cells were cultured in RPMI 1640 medium at 37 °C in 5% CO₂ supplemented with 10% fetal calf serum (FCS), Penicillin (10,000 units/ml), Streptomycin (10 mg/ml) and L-Glutamine (200 mM). The PANC-1 cells were similarly cultured except the medium was DMEM. Cells were free of *Mycoplasma* contamination as determined by a *Mycoplasma* ELISA test (Boehringer Mannheim GmbH, Mannheim, Germany) carried out every 3 months. Cell viability was determined by the SRB assay [45].

2.1.2. Chemicals

1,2-Dilauroyl-sn-Glycero-3-Phosphoethanolamine (DLPE) and 1,2-Dilauroyl-sn-Glycero-3-Glycerol (DLPG) was purchased from Avanti Polar Lipids Inc. (Alabaster, AL, USA). Hyaluronic Acid, Sodium Salt, *Streptococcus* sp., the molecular weight in the range of 5.0×10^5 – 1.2×10^6 , was obtained from Calbiochem[®] (Nottingham, UK). PTX, semisynthetic from *Taxus* sp., minimum 97%; 1-Ethyl-3-(3-dimethylamino-propyl) carbodiimide (EDAC); Sulfarhodamine B (SRB); Trichloroacetic acid (TCA); Trizma Base; Ferric chloride hexahydrate (FeCl₃·6H₂O); Ammonium thiocyanate

(NH₄SCN); Boric acid and Borax (sodium tetraborate·10H₂O) were purchased from Sigma–Aldrich Co. (St. Louis, MO, USA). ³H-PTX solv. EtOH, conc. 1 mCi/ml, SA 20 Ci/mmol and Phosphatidylethanolamine(arach-1-14C), solv. EtOH, conc. 0.1 mCi/ml, SA 55 mCi/mmol were purchased from American Radiolabeled Chemicals Inc. (St. Louis, MO, USA). Scintillation liquid, ULTIMA GOLD™ was from Perkin–Elmer Life and Analytical Sciences Inc. [11]. Materials for cell cultures were from Biological Industries Co. (Beit Haemek, Israel). Dialysis tubing (molecular weight cutoff of 12,000–14,000) was from Spectrum Medical Industries (Los Angeles, CA). Polycarbonate membranes were from Nucleopore (Pleasanton, CA). All other reagents were of analytical grade.

2.2. Methods

2.2.1. Preparation of PTX loaded-GAGs

PTX and lipids (DLPE:DLPG mole ratio of 9:1, respectively, DLPG added to assist particle homogeneity) were dissolved in ethanol separately, then mixed together. Drug loading was at 1:4 drug-lipid (w/w). The solution was evaporated to dryness under reduced pressure in a Buchi Rotary Evaporator Vacuum System (Flawil, Switzerland), and hydrated by the swelling solution that consisted of borate buffer (0.1M, pH 9). Prior to the addition of activated HA (at weight ratio of total lipid:HA 10:1 (w/w)), the suspension was heated at 45 °C for 2 h and sonicated for 10 min in a bath sonicator. HA was dissolved in acetate buffer (0.1M, pH 4.5) to a final concentration of 2 mg/ml and pre-activated by incubation with EDAC at the concentration of 40 mg/ml for 2 h at 37 °C. The activated HA was added to the lipid-drug suspension and adjusted to pH 9.0 by NaOH followed by incubation over night, at 37 °C. Excess reactive agents and by-products were removed by extensive dialysis against HBS, pH 8.2. GAGs were lyophilized and kept at –20 °C until further use. Prior to an experiment GAGs were resuspended in ddH₂O to the same pre-lyophilization volume and sonicated for 10 min using a bath sonicator. Retention of encapsulated PTX in phosphate buffer saline (PBS) and in serum (human serum:PBS 1:1 v/v) was determined by incubation in the test media at 37 °C, pulling out samples over a time span of 0–47 h, and determining the concentration of GAGs-encapsulated drug.

2.2.2. Particle size distribution and zeta potential measurements

Particle size distribution and zeta potential measurements were determined by light scattering using Malvern nano ZS Zetasizer (Worcestershire, UK). Each experimental result is an average of at least three independent measurements.

2.2.3. Ultrastructure analysis

The ultrastructure of both drug-free and PTX-containing GAGs and drug-location within the particle were investigated by environmental scanning electron microscopy (ESEM). The particles were observed using FEI Quanta 200 FEG Environmental SEM (Hillsboro, Oregon) [11], using simultaneously the Everhart–Thornley (ET) SE detector and the STEM detector at primary beam energy of 20 keV. Drops of prepared aqueous samples diluted 1:5 were placed on holey carbon grid. After air-drying the drop was viewed under an electron microscope in STEM mode and photographed.

2.2.4. Thermal analysis

Differential Scanning Calorimetry (DSC) and Thermo-gravimetric Analysis (TGA) using analyzers of TA Instruments SDT 2920 and SDT 2960 (Eschborn, Germany)/Hi [11] respectively, were performed with dry (lyophilized) samples for drug-free GAGs, PTX-GAGs and the mixture of empty GAGs and crystalline PTX at the same weight ratio as the TX/GAG particles. Heating rate was 10 °C/min from room temperature to 350 °C.

2.2.5. Quantitative determinations

PTX and DLPE were determined by including trace amounts of ³H-Paclitaxel and ¹⁴C-phosphatidylethanolamine in all PTX-PE-containing systems. An additional method for PE quantifying was optic assay based on formation of DLPE-ammonium ferriothiocyanate complex extracted to chloroform phase and measured at 470 nm [46]. Briefly, first, aqueous solution of reagent, containing ferric chloride hexahydrate (FeCl₃·6H₂O) and ammonium thiocyanate (NH₄SCN) at concentrations of 27 g/l and 30 g/l respectively, was prepared. Preparation of test and standard samples were performed in the following manner: a small volume of DLPE suspension (20–200 μl) was added to 2 ml of chloroform, mixed, and 1 ml of reagent was added. Mixed systems were separated then to two phases (organic and aqueous) by low speed centrifugation. The organic phase, as aforesaid, was taken for absorption measurement at 470 nm.

2.2.6. Binding assay

CT-26 cells were washed twice with PBS and incubated with Alexa Fluor 488 anti-CD44 Rat anti-mouse (clone 1M7, Biogenet) on ice for 30 min followed by washing with PBS and subjecting to flow cytometry (FACSCalibur, Franklin Lakes, NJ).

2.2.7. *In vitro* cytotoxicity

CT-26 cells were cultured in RPMI 1640 medium containing 1.5 mM L-glutamine, 10% FBS and 1% PSN. 24 h prior to treatment, the cells were seeded in 96-

well plates, 100 μ l/well, at 5×10^4 /ml. The treatment was initiated on non-confluent cell layers by adding 25 μ l/well of the test samples and controls and termination was 72 h later. Cell proliferation upon termination was determined by the SRB method [45].

2.2.8. Blood biomarker assay

Healthy BALB/c mice ($n = 4$ /group) were given four once-per-week bolus i.v. injections of saline, or treated with drug-free GAGs, PTX-Cre or PTX-GAGs. At day 24 post initial injection, blood was drawn and the serum was obtained by centrifugation of the whole blood at 3000 rpm for 15 min. Liver enzyme levels of Alanine Aminotransferase (ALT) and Aspartate Aminotransferase (AST) were determined by COBAS MIRA auto analyzer (Roche, Nutley, New Jersey).

2.2.9. Isolation of PBMC and interferon assay

Mononuclear cells were isolated from the spleen as previously described [35]. Expression of IFN or interferon responsive genes was examined by quantitative RT-PCR. IFN β , OAS1 and STAT1 primers were as previously described [35].

2.2.10. Cytokine induction

Mice splenocytes were isolated from the spleen as previously described [35]. The cells (2×10^5 cells in a well of 24 well) were treated with saline, drug-free GAGs, PTX-Cre and PTX-GAGs at a dose 2.5 μ M PTX for 24 h. Cytokines mRNA were examined using quantitative RT-PCR (One step plus, ABI) with the following primers: GAPDH, IL-2, TNF α , and IFN γ as previously reported [35].

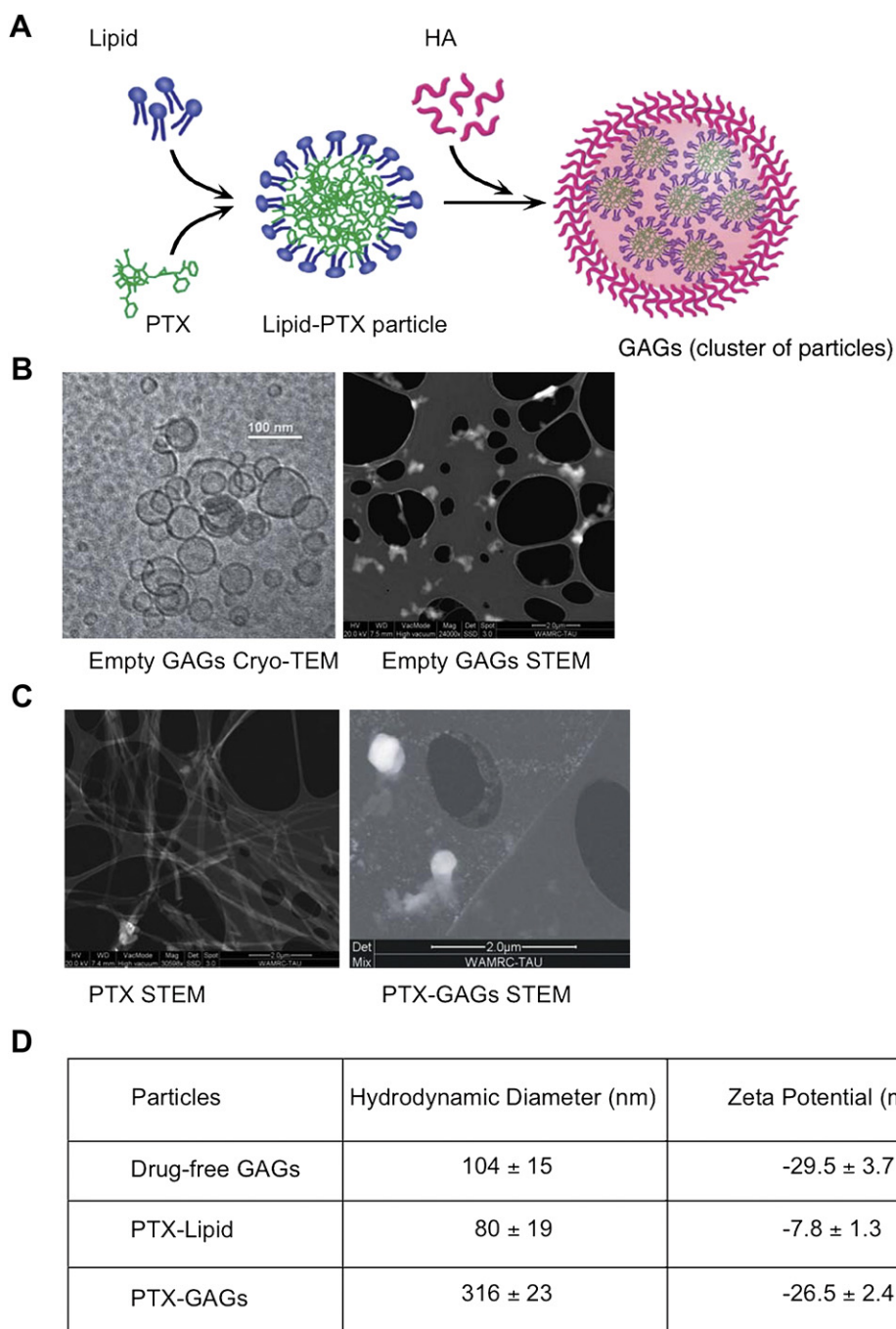


Fig. 1. PTX-GAG's structural and physicochemical properties. (A) A schematic illustration of the process involved in generating PTX-GAGs. Lipids are mixed with PTX to form lipid-PTX particles that cluster together and are subsequently coated with HA to form the GAGs. (B) Representative images of the ultrastructure of drug-free GAGs using Cryo-TEM (left panel) and STEM (right panel) show the globular shape of the particles. (C) STEM images of PTX (left panel) and of PTX-GAGs (right panel) show free PTX's fiber-like structure and the condensed round-shape of the particles. (D) Hydrodynamic diameters and zeta potential measurements of drug-free GAGs, lipid-PTX particles and PTX-GAGs support the clustering structure that is stabilized by the HA coating. Data are expressed as the mean \pm SD of at least three independent experiments.

2.2.11. Quantitative RT-PCR

Quantitative RT-PCR using a Step one Plus Real-time RT-PCR (ABI, Foster City, CA) was carried out as previously described [35]. Primers for mouse GAPDH, STAT1, OAS1, IFN β , IL-2, TNF α , and IFN γ were used as previously described [35]. The following primer pairs were used: IL-6 primers: forward primer: 5'-ATCCAGTTGCCTTCTTGG-GACTGA-3'; reverse primer: 5'-TAAGCCTCCGACTTGTGAAGTGGT-3'. All primers were synthesized by Syntheza Inc. (Rehovot, Israel).

2.2.12. CT-26, colon adenocarcinoma-bearing mice model

All animal experiment protocols were approved by the Institutional Review Board at the Immune Disease Institute. The model was established as previously reported [19]. PTX-GAGs and drug-free GAGs were tested in this model to examine their pharmacokinetics and tissue distribution, efficacy and unwanted immune response. All the experimental details are listed in the main text and figures.

2.2.13. Statistical analysis

In vitro data were analyzed using Student's *t*-test. Differences between treatment groups were evaluated by one-way ANOVA with significance determined by Bonferroni adjusted *t*-tests.

3. Results and discussion

3.1. Structural and physicochemical characterization of drug-free and PTX-loaded particles

The steps in forming the PTX-GAG particles are illustrated in Fig. 1A (drug-free GAGs are prepared quite similarly, except the omission of drug). As described under methods and demonstrated in Fig. 1A, GAGs are composed of the lipid molecules that self-assemble into particulate clusters (with/without PTX), that are then covalently coated with high-molecular weight HA at a lipid:HA ratio of 10:1 (w/w). HA is the main component of the particle's surface and its interior contains both the lipid clusters and water regions, providing an intrinsic ability to accommodate both hydrophilic and hydrophobic drugs.

The PTX-lipid clusters, drug-free GAGs and PTX-GAGs have globular shapes as evidenced by cryo-TEM and STEM images (Fig. 1B, C right panel) with mean diameters of 80, 100 and 300 nm, respectively (Fig. 1D), whereas PTX alone forms long strings (Fig. 1C left panel). Zeta potential measurements support the lipid cluster tendency with a value of about -8 mV (Fig. 1D), while coating the PTX-lipid particulate cluster with HA stabilizes the structure (Fig. 1C right panel) with a zeta potential of -27 mV (Fig. 1D). Over the PTX:lipid ratio range of 1:4 to 1:1 drug encapsulation efficiency was high (approaching 100%). There was no loss of encapsulated PTX over the time span of 47 h, whether the particles were suspended in buffer alone (PBS) or in PBS: serum (1:1. v/v).

3.2. Thermal analysis of PTX-GAGs

PTX in aqueous systems is in the form of precipitating crystals (dry or hydrated), and is expected to take an amorphous-like form upon incorporation/dispersion within a particle such as the GAGs [47]. It has been shown that subjecting free crystalline PTX (dry or hydrated) to differential scanning calorimetry (DSC) results in an endothermic peak at the temperature range of 220 °C followed immediately by an exothermic peak. With the aid of thermogravimetric analysis (TGA) peak assignments are melting for the first peak, and decomposition for the second one. In contrast, it was shown that free amorphous PTX has only the decomposition peak, slightly-shifted to lower temperatures (~ 5 – 10 °C) compared to the crystalline material [47]. These assumptions were used for this study.

DSC studies (Fig. 2A) showed that the crystalline PTX (Fig. 2A(1)) had, as expected, an endothermic peak in the range of 220 °C followed immediately by an exothermic peak, identified through TGA (Fig. 2B) as melting and decomposition, respectively. Drug-free

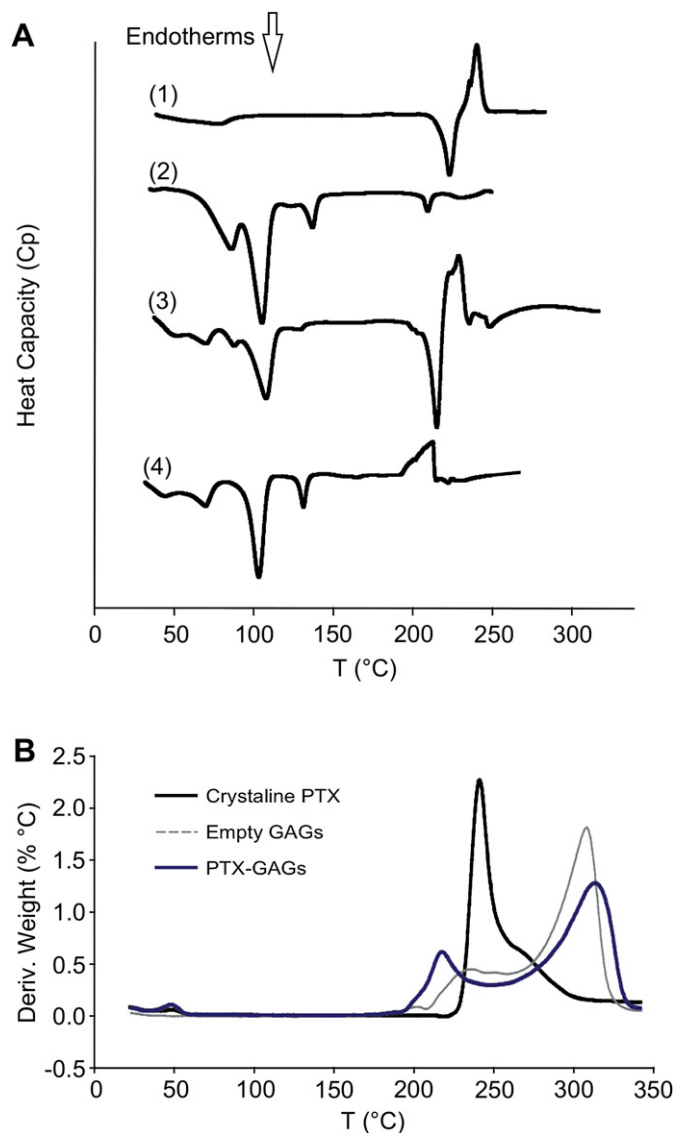


Fig. 2. Thermal analysis of PTX-GAGs. (A) Representative curves of Differential Scanning Calorimetry (DSC) (1) Crystalline PTX (2) Drug-free GAGs (3) A mixture of crystalline PTX with drug-free GAGs and (4) PTX-GAGs. (B) Representative thermogravimetric (TGA) curves of pure PTX, drug-free and PTX-containing GAGs are overlaid in the figure. Each value represents at least 3 independent experiments.

GAGs had no significant energy consumption or release at the regions relevant for the drug (Fig. 2A (2)). Mixtures of drug-free GAGs and (external) crystalline PTX, showed the peaks typical to the thermogram of each component separately (Fig. 2A (3)). The thermogram of PTX-GAG retained the GAG pattern and showed a single PTX peak – the decomposition (Fig. 2A (4), B) indicating that, in the PTX-GAGs, PTX was in a condition typical to its amorphous structure [14]. These findings strongly support the assignment that, in the GAGs system, PTX resides within the particle.

3.3. GAGs binding to CD44-expressing colorectal cancer cells

CD44 has been extensively studied by our group and others, as a receptor target for drug delivery [19,20,22]. We have chosen the mouse colorectal carcinoma cell line CT-26, that expresses CD44 as our model system for exploring GAGs' ability to deliver PTX to CD44-expressing tumors. We first studied CD44 expression in CT-

26 cells using flow cytometry. Upon confirming CD44 expression on CT-26 cells (Fig. 3A) we tested if GAGs can bind to CD44, while competing with a monoclonal antibody [28] raised against mouse CD44 on the receptor's binding site (Fig. 3B). GAGs were incubated with the cells, and at 0.5, 6 and 12 h post incubation, an anti-mouse CD44 mAb was added and the cells were subjected to flow cytometry. Thirty minutes of GAGs' incubation with the cells sufficed to completely abolish the binding of mAb against CD44 (Fig. 3B), taking up to 12 h to get back to original anti-CD44 binding levels, supporting the hypothesis that GAGs operates in a CD44-dependent manner. Six hours post incubation, binding of anti-CD44 was about half of its binding capacity (Fig. 3B) suggesting that GAGs are beginning to be cleared from the receptor's binding region within 6 h post incubation and complete their clearance within 12 h post incubation.

CD44-GAG interactions are not restricted to colorectal cancer cells, as demonstrated (Supplementary Fig. 1) for D122 (mouse lung carcinoma), and for PANC-1 (human pancreatic adenocarcinoma) cells. Negligible doxorubicin accumulation was observed upon 1 h of free drug incubation with D122 cells, whereas similar incubation with GAG-encapsulated doxorubicin resulted in substantial intracellular drug accumulation. (Supplementary Fig. 1A). Double-

labeled GAGs (surface and interior) provided further details. Under the conditions described above for doxorubicin, both surface and interior markers are seen inside the cells (Supplementary Fig. 1B). Including the energy inhibitor 2-Deoxyglucose (2-DOG) in the incubation medium generated a significant reduction in cell-associated GAGs, most of the remaining particles localizing at the cell surface (Supplementary Fig. 1C). Several potential mechanisms are postulated such as particle internalization, or conformational changes in the GAGs that open the structure and facilitate entry of its interior components into the cells. These mechanisms are of great interest and are currently under investigation in our groups and are, thus, beyond the scope of the research described in this manuscript.

3.4. GAGs-mediated PTX delivery to colorectal cancer cells

We next examined the *in vitro* cytotoxicity of PTX-GAGs compared to free PTX. PTX cytotoxicity was not impaired upon entrapment in the GAGs (PTX-GAGs) and was on a par with that of free PTX, with an IC_{50} of $\sim 0.16 \mu\text{M}$ (Fig. 3C). It is likely that PTX-GAGs will have more profound effects *in vivo* than *in vitro*, taking into account the random distribution of the free form of PTX versus PTX-GAGs that should accumulate in CD44-expressing tumors.

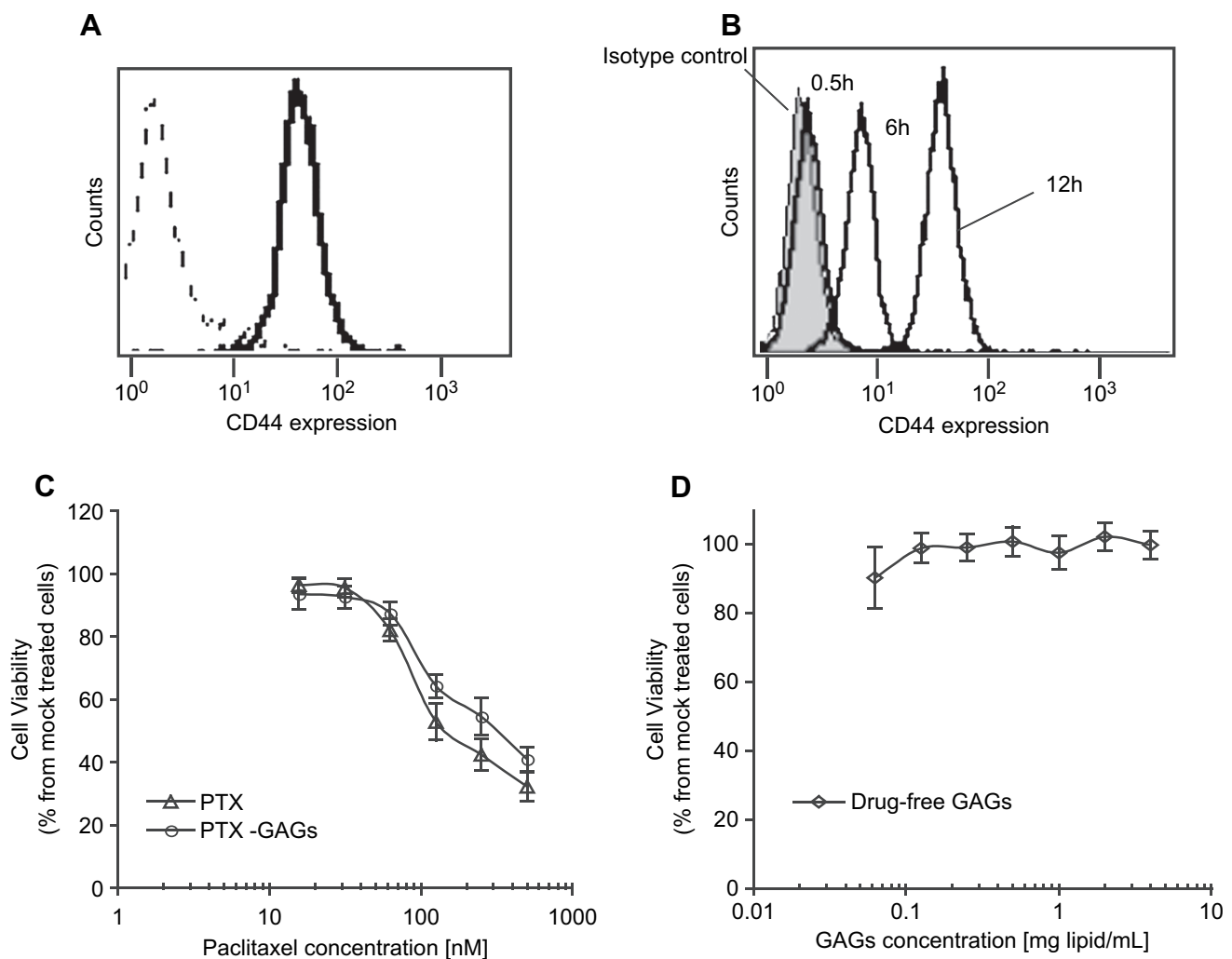


Fig. 3. GAGs bind and deliver PTX to colorectal cancer cells (CT-26) in a CD44-dependent manner. (A) Representative histogram of CD44 expression in CT-26 cells determined by immunofluorescent cytometry. Dash line – isotype control; solid line – anti-CD44 monoclonal antibody (28). (B) Competitive assay showing the complete blocking of CD44 by drug-free GAGs (5 µg/mL). The blocking effect lasts up to 12 h as evident by the recovered CD44 expression (assayed by an anti-CD44 mAb). (C, D) Cell viability assay of PTX vs. PTX-GAGs or drug-free GAGs. Data are expressed as the mean \pm SD of at least three independent experiments, six repeats per data point in each experiment.

Drug-free GAGs had no impact on cell viability (Fig. 3D), supporting the hypothesis that GAGs per se will not induce any cell death given that they are composed from natural materials that are recognized as 'self'. In addition, sterilization conditions (autoclave at 121 °C for 12 min) and downsizing GAGs by sonication also had no detrimental effect on drug activity (data not shown).

3.5. Evaluation of serum liver enzymes and weight changes after intravenous GAGs administration

Serum levels of the transaminases liver enzymes such as alanine aminotransferase (ALT) and aspartate aminotransferase (AST) are respectively regarded as reliable indicators of liver tissue damage and, more general, systemic tissue damage [48]. We examined the release of liver enzymes and changes in body weight of healthy BALB/c mice treated with PTX-GAGs. Mice ($n = 4/\text{group}$) were given four weekly bolus intravenous (i.v.) injections of either the conventional PTX formulation (i.e. PTX-Cre) in saline, or the PTX-GAGs particles suspended in saline, both at the dose of 5 mg PTX/Kg body. Mock treated (saline) and drug-free GAGs (same particle dose as those formulated with PTX) served as controls. Blood samples

were taken 2 days after the 4th and final dose (day 24). PTX-GAGs induced only mild changes, that are considered well tolerated, in liver enzymes (Fig. 4A) [49]. PTX-Cre released high amounts of liver enzymes indicating possible liver damage upon multiple i.v. injections (Fig. 4A). A change in body weight is also considered as a global toxicity marker [35]. Mice ($n = 5/\text{group}$) were given four bolus i.v. injections of the designated formulations (as indicated in Fig. 4B) and changes in body weight were observed up to 24 days. PTX-GAGs were well tolerated and did not cause any significant decrease in mice body weight (Fig. 4B). Mice treated with PTX-Cre lost body weight (up to 5% at day 24) and the injections were followed by shivering that lasted 20 min (data not shown). We have not observed this behavior pattern when mice were injected with drug-free GAGs or PTX-GAGs. Thus, formulating PTX in GAGs does not releasing liver enzymes and is well tolerated upon multiple i.v. injections.

3.6. Evaluation of interferon response and of cytokine induction after intravenous GAGs administration

A possible adverse effect of delivery systems is the activation of interferon (IFN)-responsive genes (IRG) by activating protein kinase

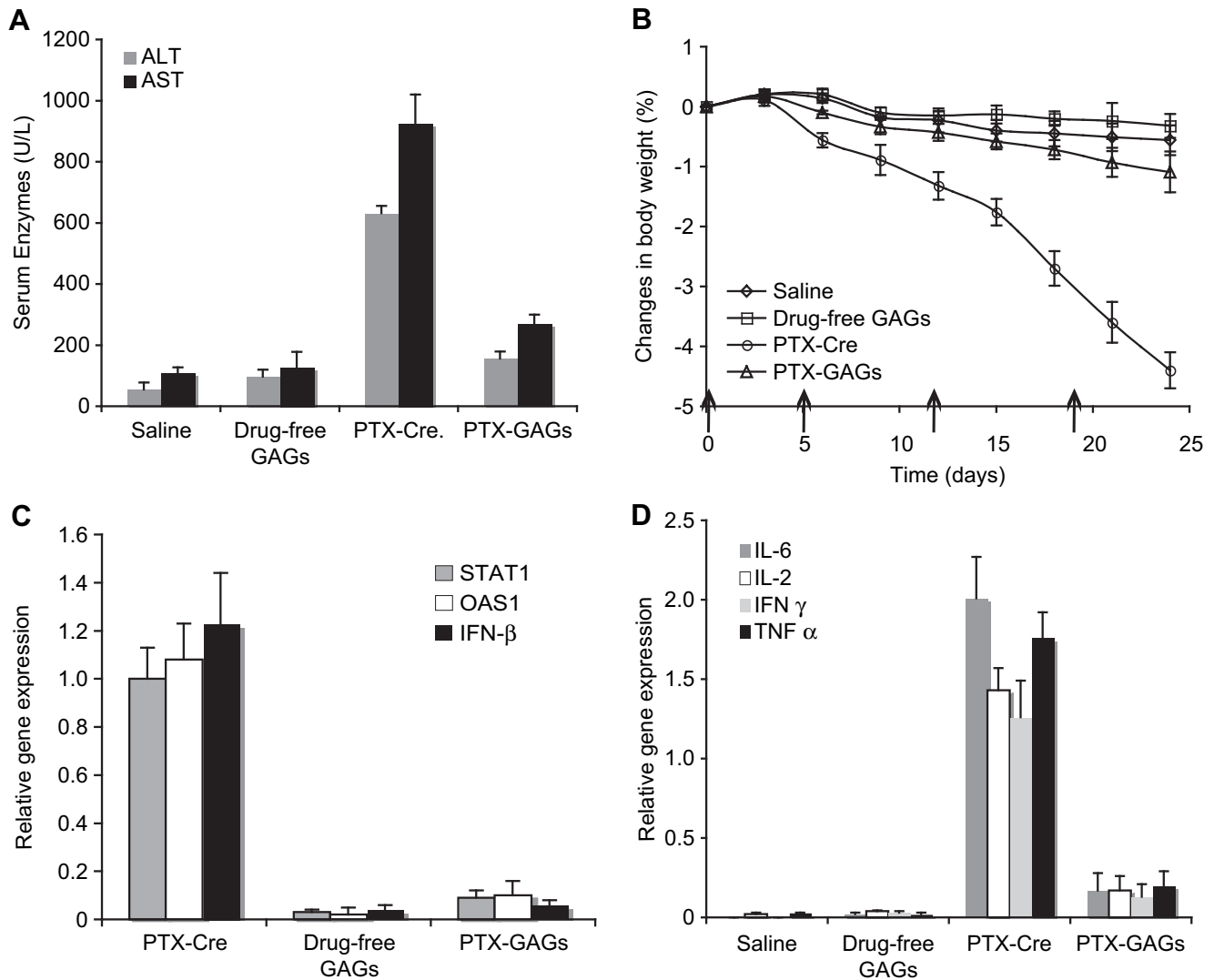


Fig. 4. GAGs do not induce adverse effects. (A) ALT and AST liver enzyme levels were examined 24 days after 4 weekly bolus injections into healthy BALB/c mice ($n = 4/\text{group}$). (B) Changes in body weight were monitored over a period of 24 days after 4 i.v. bolus injections ($n = 5/\text{group}$) (C) Activation of interferon response studied in PBMC using quantitative real-time RT-PCR. (D) mRNA levels of cytokines were measured using quantitative real-time RT-PCR. Data are expressed as mean \pm SEM of at least three independent experiments.

PKR or by binding to toll-like receptors. To examine whether GAGs activate an IFN response, we used quantitative RT-PCR to measure mRNA expression of IFN β , and two key IRG 2',5'-oligoadenylate synthetase 1 (OAS1) and STAT1 in mice peripheral blood mononuclear cells (PBMC) stimulated with $Mg^{2+}/EGTA$ [35] and then treated with GAGs. Treatment with drug-free GAGs and PTX-GAGs (Fig. 4C) did not induced any IFN response, whereas treatment with PTX-Cre (Fig. 4C) induced a high response similar to induction with known IFN inducers such as lipopolysaccharides (LPS) (data not shown). This could be attributed to the presence of Cremophor[®] EL (polyoxyethylated castor oil) and ethanol (CrEL) solvent, that are known to affect many types of immune cells, among them mast

cells that secrete histamine during treatment with PTX formulated in CrEL [4].

Cytokine induction (mainly pro-inflammatory cytokines) is considered a known unwanted adverse effect of many delivery systems [50]. To examine if GAGs induce cytokines, we used quantitative RT-PCR to measure mRNA expression of the pro-inflammatory cytokines interleukin-2 (IL-2), interferon γ (IFN γ), tumor necrosis α (TNF α) and the inflammatory marker interleukin 6 (IL-6) in mice splenocytes treated with GAGs. Drug-free GAGs did not induced cytokines and were barely detected compare to mouse GAPDH (Fig. 4D). PTX-Cre induced very high levels of mRNA of all the tested cytokines and mainly IL-6 (a marker for global

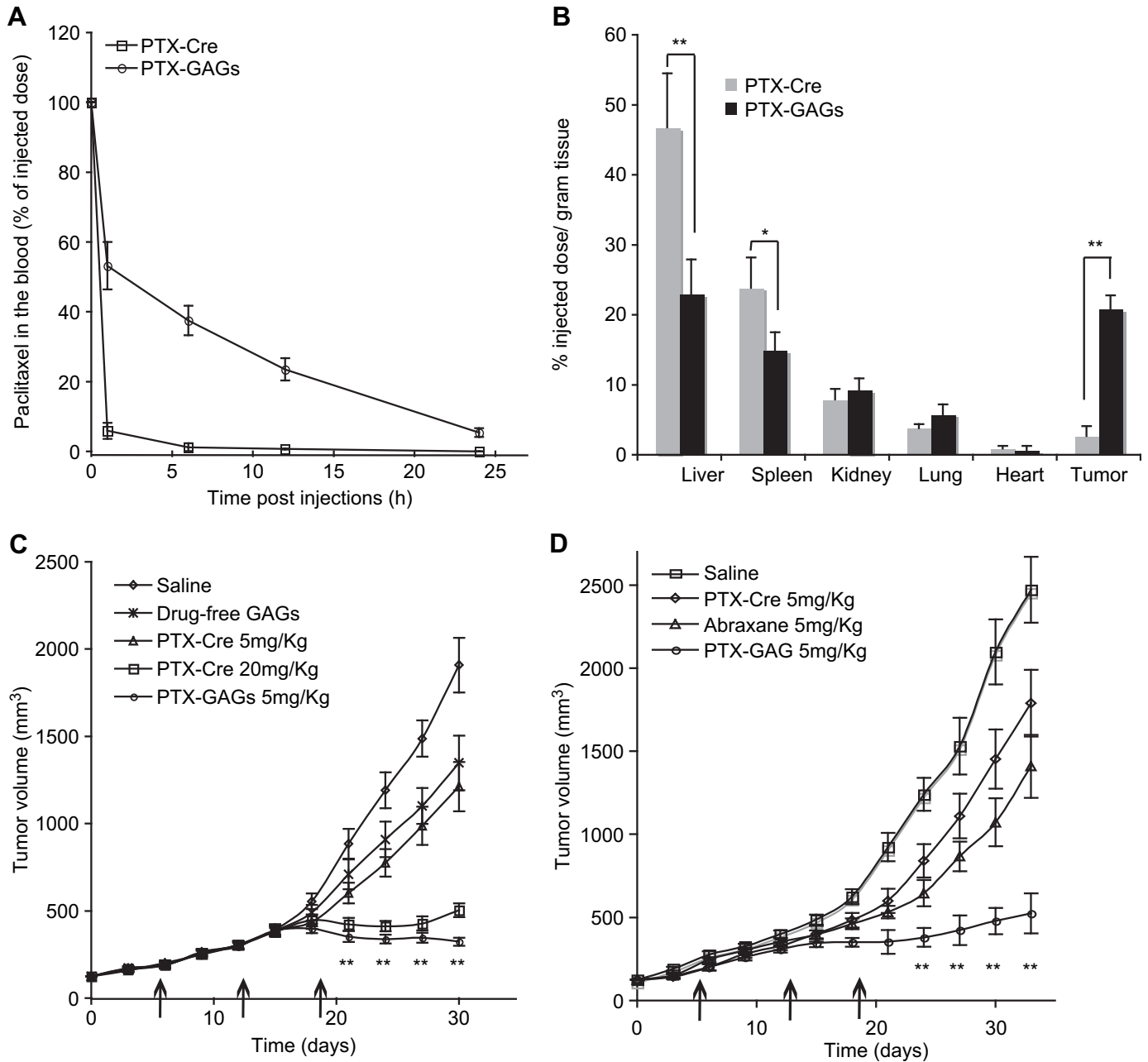


Fig. 5. PTX-GAGs act as tumor-targeted, long circulating particles with robust anti-tumor activity. (A, B) PTX pharmacokinetics studied using radiolabeled PTX. BALB/c mice ($n = 10$ /group) bearing CT-26 tumors were injected with PTX-Cre or PTX-GAGs at 5 mg/Kg body 21 days from tumor initiation. PTX-GAGs were long circulating with half-life of ~ 6 h compared to 10 min in the PTX-Cre. Reduction in liver and spleen uptake was observed with the PTX-GAGs vs. PTX-Cre. High accumulation of PTX in the tumor was observed when delivered as PTX-GAGs compared to low accumulation when delivered as PTX-Cre. (C, D) Therapeutic efficacy was demonstrated using 3 i.v. bolus injections at days 5, 12, and 19 post initiation of the experiment with doses and formulations as listed. Data are expressed as the mean \pm SEM of 3 independent experiments ($n = 7$ /group/experiment) $p < 0.05^*$; 0.01^{**} vs. PTX-Cre treatment.

inflammation) and TNF (Fig. 4D) supporting the known effect of CrEL on immune cells (4). PTX-GAGs elucidated very mild response that was 5-fold less than the FDA-approved formulation of PTX-Cre. Therefore, even in highly sensitive primary immune cells, GAGs are acting as a shield from triggering an IFN response or inducing pro-inflammatory cytokines.

3.7. Pharmacokinetics, biodistribution and therapeutic responses in tumor-bearing mice treated with PTX-GAGs

Coating particles with long circulating agents such as PEG or HA contributes to steric stabilization of the vesicles and provides protection from opsonization, which is an essential desirable property in drug delivery [21]. We examined the pharmacokinetics and biodistribution of PTX formulated either in CrEL (i.e. PTX-Cre) or in GAGs, in mice bearing CT-26 tumors. BALB/c mice ($n = 10/\text{group}$) bearing CT-26 tumors were injected with PTX-Cre or PTX-GAGs at 5 mg/Kg body 21 days from tumor initiation. PTX-Cre was eliminated from the circulation within less than 1 h post i.v. injection (Fig. 5A). PTX-GAGs were still circulating even 24 h post i.v. injection, which provided another layer of support that HA is coating the PTX-lipid particles (Fig. 5A). The biodistribution of PTX in tissues was assayed 24 h post injection to mice ($n = 7/\text{group}$) bearing CT-26 tumors. PTX-GAGs reduced PTX liver and spleen accumulation by almost 2-fold, and increased PTX accumulation in the tumor by 10-fold compared with the PTX-Cre formulation (Fig. 5B).

Therapeutic responses to iv-administered PTX-GAGs, Taxol[®] (PTX-Cre) and Abraxane[®] were studied in tumor-bearing (CT-26) mice. Tumor progression was exponential, tumor volumes increasing 9–17 fold over a 30 day period, in mice receiving saline, drug-free GAGs, 5 mg/Kg body Taxol[®] or 5 mg/Kg body Abraxane[®] (Fig. 3C, D). In similar treatment with 5 mg/Kg body PTX-GAGs, tumor progression was arrested (Fig. 3C, D) and this treatment was as potent as 20 mg/Kg body Taxol[®]. (Fig. 3C). Mice receiving this high Taxol[®] dose experienced 20 min shivering during the i.v. administration and 7.3% loss of body weight (data not shown) indicating global toxicity that not seen with the GAGs formulation.

4. Conclusions

We devised a strategy that utilized taxanes' affinity to lipids, to self-assemble into nanoparticle-like clusters and then, by covalently binding them to HA, we further exploited the interaction between the HA-coated particles and CD44 on tumor cells. PTX was chosen as a proof-of-principle and was formulated in the GAGs (PTX-GAGs). We found this system to be superior to the FDA-approved formulations in improved efficacy (even at 4-fold lower doses), and in reduced unwanted adverse effects. These findings suggest that GAGs merit further investigation as nanovectors for insoluble drugs and may be applicable as carriers in other therapeutic settings.

Acknowledgements

We declare no conflict of interests. This work was supported by grants from the Alon Foundation, the Marie Curie IRG-FP7 of the European Union, and the Lewis family-trust for cancer research to Dan Peer.

Appendix. Supplementary material

The supplementary data associated with this article can be found in the on-line version at doi:10.1016/j.biomaterials.2010.05.067.

Appendix

Figures with essential color discrimination. Figs. 1 and 2 in this article are difficult to interpret in black and white. The full color images can be found in the on-line version, at doi:10.1016/j.biomaterials.2010.05.067.

References

- [1] Panchagnula R. Pharmaceutical aspects of paclitaxel. *Int J Pharm* 1998;172:1–15.
- [2] Singla AK, Garg A, Aggarwal D. Paclitaxel and its formulations. *Int J Pharm* 2002;235(1–2):179–92.
- [3] Fetterly GJ, Straubinger RM. Pharmacokinetics of paclitaxel-containing liposomes in rats. *AAPS PharmSci* 2003;5(4):E32.
- [4] Friedland D, Gorman G, Treat J. Hypersensitivity reactions from taxol and etoposide. *J Natl Cancer Inst* 1993;85(24):2036.
- [5] Lilley LL, Scott HB. What you need to know about taxol. *Am J Nurs* 1993;93(12):46–50.
- [6] Gelderblom H, Verweij J, Nooter K, Sparreboom A, Cremophor EL. The drawbacks and advantages of vehicle selection for drug formulation. *Eur J Cancer* 2001;37(13):1590–8.
- [7] Weiss RB, Donehower RC, Wiernik PH, Ohnuma T, Gralla RJ, Trump DL, et al. Hypersensitivity reactions from taxol. *J Clin Oncol* 1990;8(7):1263–8.
- [8] Gianni L, Kearns CM, Giani A, Capri G, Viganò L, Lacatelli A, et al. Nonlinear pharmacokinetics and metabolism of paclitaxel and its pharmacokinetic/pharmacodynamic relationships in humans. *J Clin Oncol* 1995;13(1):180–90.
- [9] Bernsdorff C, Reszka R, Winter R. Interaction of the anticancer agent taxol (paclitaxel) with phospholipid bilayers. *J Biomed Mater Res* 1999;46(2):141–9.
- [10] Campbell RB, Balasubramanian SV, Straubinger RM. Influence of cationic lipids on the stability and membrane properties of paclitaxel-containing liposomes. *J Pharm Sci* 2001;90(8):1091–105.
- [11] Crossasso P, Ceruti M, Brusa P, Arpicco S, Dosio F, Cattel L. Preparation, characterization and properties of sterically stabilized paclitaxel-containing liposomes. *J Control Release* 2000;63(1–2):19–30.
- [12] Sharma A, Straubinger RM. Novel taxol formulations: preparation and characterization of taxol-containing liposomes. *Pharm Res* 1994;11(6):889–96.
- [13] Wenk MR, Fahr A, Reszka R, Seelig J. Paclitaxel partitioning into lipid bilayers. *J Pharm Sci* 1996;85(2):228–31.
- [14] Zhao L, Feng SS, Go ML. Investigation of molecular interactions between paclitaxel and DPPC by langmuir film balance and differential scanning calorimetry. *J Pharm Sci* 2004;93(1):86–98.
- [15] Hawkins MJ, Soon-Shiong P, Desai N. Protein nanoparticles as drug carriers in clinical medicine. *Adv Drug Deliv Rev* 2008;60(8):876–85.
- [16] Green MR, Manikhas GM, Orlov S, Afanasyev B, Makhson AM, Bhar P, et al. Abraxane(R), a novel cremophor(R)-free, albumin-bound particle form of paclitaxel for the treatment of advanced non-small-cell lung cancer. *Ann Oncol* 2006;17(8):1263–8.
- [17] Matsumura Y, Maeda H. A new concept for macromolecular therapeutics in cancer chemotherapy: mechanism of tumor-tropic accumulation of proteins and the antitumor agent smancs. *Cancer Res* 1986;46(12 Pt 1):6387–92.
- [18] Maeda H, Sawa T, Konno T. Mechanism of tumor-targeted delivery of macromolecular drugs, including the EPR effect in solid tumor and clinical overview of the prototype polymeric drug SMANCS. *J Control Release* 2001;74(1–3):47–61. 6.
- [19] Peer D, Margalit R. Tumor-targeted hyaluronan nanoliposomes increase the antitumor activity of liposomal doxorubicin in syngeneic and human xenograft mouse tumor models. *Neoplasia* 2004;6(4):343–53.
- [20] Peer D, Margalit R. Loading mitomycin c inside long circulating hyaluronan targeted nano-liposomes increases its antitumor activity in three mice tumor models. *Int J Cancer* 2004;108(5):780–9.
- [21] Peer D, Karp JM, Hong S, Farokhzad OC, Margalit R, Langer R. Nanocarriers as an emerging platform for cancer therapy. *Nat Nanotechnol* 2007;2(12):751–60.
- [22] Platt VM, Szoka Jr FC. Anticancer therapeutics: targeting macromolecules and nanocarriers to hyaluronan or CD44, a hyaluronan receptor. *Mol Pharm* 2008;5(4):474–86.
- [23] Lapcik Jr L, Lapcik L, De Smedt S, Demeester J, Chabreck P. Hyaluronan: preparation, structure, properties, and applications. *Chem Rev* 1998;98(8):2663–84.
- [24] O'Regan M, Martini I, Crescenzi F, De Luca C, Lansing M. Molecular mechanisms and genetics of hyaluronan biosynthesis. *Int J Biol Macromol* 1994;16(6):283–6.
- [25] Yerushalmi N, Arad A, Margalit R. Molecular and cellular studies of hyaluronic acid-modified liposomes as bioadhesive carriers for topical drug delivery in wound healing. *Arch Biochem Biophys* 1994;313(2):267–73.
- [26] Yerushalmi N, Margalit R. Hyaluronic acid-modified bioadhesive liposomes as local drug depots: effects of cellular and fluid dynamics on liposome retention at target sites. *Arch Biochem Biophys* 1998;349(1):21–6.

- [27] Birch M, Mitchell S, Hart IR. Isolation and characterization of human melanoma cell variants expressing high and low levels of CD44. *Cancer Res* 1991;51(24):6660–7.
- [28] Penno MB, August JT, Baylin SB, Mabry M, Linnoila RI, Lee VS, et al. Expression of CD44 in human lung tumors. *Cancer Res* 1994;54(5):1381–7.
- [29] Bartolozzi A, Peach R, Aruffo A, Stamenkovic I. Interaction between CD44 and hyaluronate is directly implicated in the regulation of tumor development. *J Exp Med* 1994;180(1):53–66.
- [30] Guo Y, Ma J, Wang J, Che X, Narula J, Bigby M, et al. Inhibition of human melanoma growth and metastasis in vivo by anti-CD44 monoclonal antibody. *Cancer Res* 1994;54(6):1561–5.
- [31] Zeng C, Toole BP, Kinney SD, Kuo JW, Stamenkovic I. Inhibition of tumor growth in vivo by hyaluronan oligomers. *Int J Cancer* 1998;77(3):396–401.
- [32] Chen WY, Abatangelo G. Functions of hyaluronan in wound repair. *Wound Repair Regen* 1999;7(2):79–89.
- [33] Peer D, Florentin A, Margalit R. Hyaluronan is a key component in cryoprotection and formulation of targeted unilamellar liposomes. *Biochim Biophys Acta* 2003;1612(1):76–82.
- [34] Eliaz RE, Szoka Jr FC. Liposome-encapsulated doxorubicin targeted to CD44: a strategy to kill CD44-overexpressing tumor cells. *Cancer Res* 2001;61(6):2592–601.
- [35] Peer D, Park EJ, Morishita Y, Carman CV, Shimaoka M. Systemic leukocyte-directed siRNA delivery revealing cyclin D1 as an anti-inflammatory target. *Science* 2008;319(5863):627–30.
- [36] Barkay Z, Rivkin I, Margalit R. Three-dimensional characterization of drug-encapsulating particles using STEM detector in FEG-SEM. *Micron* 2009;40(4):480–5.
- [37] Cullis PR, de Kruijff B. Lipid polymorphism and the functional roles of lipids in biological membranes. *Biochim Biophys Acta* 1979;559(4):399–420.
- [38] Groves MJ, Herman CJ. The redistribution of bulk aqueous phase phospholipids during thermal stressing of phospholipid-stabilized emulsions. *J Pharm Pharmacol* 1993;45(7):592–6.
- [39] Hui SW, Viswanathan R, Zasadzinski JA, Israelachvili JN. The structure and stability of phospholipid bilayers by atomic force microscopy. *Biophys J* 1995;68(1):171–8.
- [40] Hyde ST. Identification of lyotropic liquid crystalline mesophases. In: Holmberg K, editor. *Handbook of applied surface and colloidal chemistry*. John Wiley & Sons, Ltd; 2001. p. 299–332 [Chapter 16].
- [41] Koyanova R, Tenchov B, Rapp G. Effect of PEG-lipid conjugates on the phase behavior of phosphatidylethanolamine dispersions. *Colloids Surf* 1999;149:571–5.
- [42] Seddon JM, Templer RH. Polymorphism of lipid-water systems. In: Lipowsky R, Sackman E, editors. *Handbook of biological physics*, vol 1. Elsevier science B.V; 1995. p. 99–159 [Chapter 3].
- [43] Seddon JM, Harlos K, Marsh D. Metastability and polymorphism in the gel and fluid bilayer phases of dilauroylphosphatidylethanolamine. Two crystalline forms in excess water. *J Biol Chem* 1983;258(6):3850–4.
- [44] Zhao L, Feng SS. Effects of lipid chain length on molecular interactions between paclitaxel and phospholipid within model biomembranes. *J Colloid Interface Sci* 2004;274(1):55–68.
- [45] Papazisis KT, Geromichalos GD, Dimitriadis KA, Kortsaris AH. Optimization of the sulforhodamine B colorimetric assay. *J Immunol Methods* 1997;208(2):151–8.
- [46] Stewart JC. Colorimetric determination of phospholipids with ammonium ferrothiocyanate. *Anal Biochem* 1980;104(1):10–4.
- [47] Liggins RT, Hunter WL, Burt HM. Solid-state characterization of paclitaxel. *J Pharm Sci* 1997;86(12):1458–63.
- [48] Injac R, Perse M, Obermajer N, Djordjevic-Milic V, Prijatelj M, Djordjevic A, et al. Potential hepatoprotective effects of fullerol C60(OH)24 in doxorubicin-induced hepatotoxicity in rats with mammary carcinomas. *Biomaterials* 2008;29(24–25):3451–60.
- [49] Akinc A, Goldberg M, Qin J, Dorkin JR, Gamba-Vitalo C, Maier M, et al. Development of Lipidoid-siRNA formulations for systemic delivery to the liver. *Mol Ther* 2009;17(5):872–9.
- [50] Peer D, Shimaoka M. Systemic siRNA delivery to leukocyte-implicated diseases. *Cell Cycle* 2009;8(6):853–9.